Supplementary Figure 1

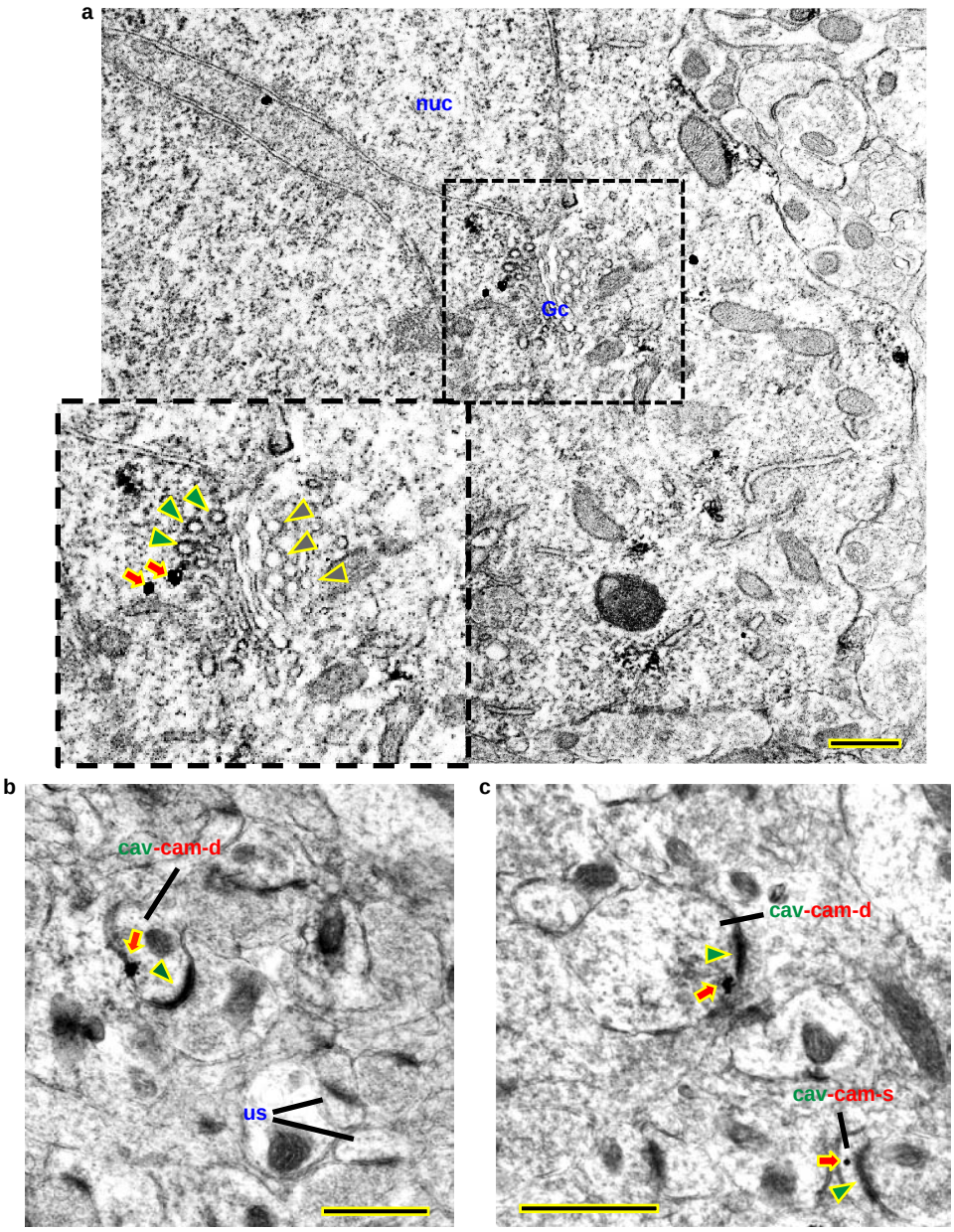

Supplementary Figure 2

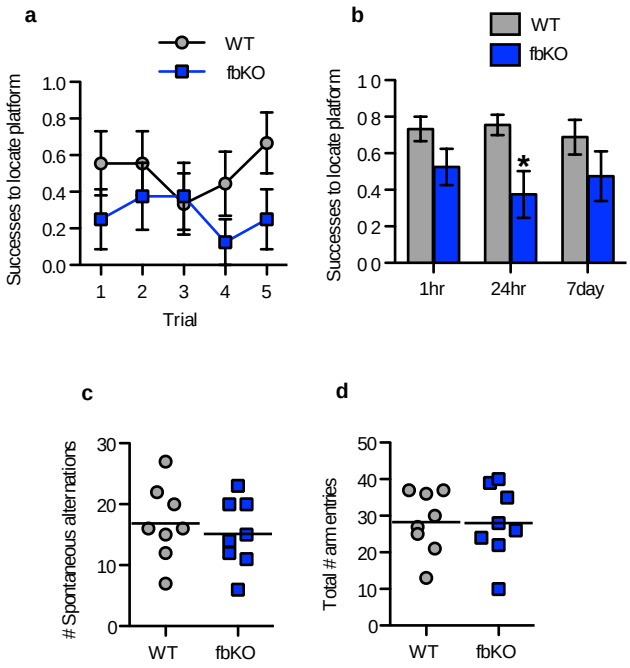

Supplementary Figure 3

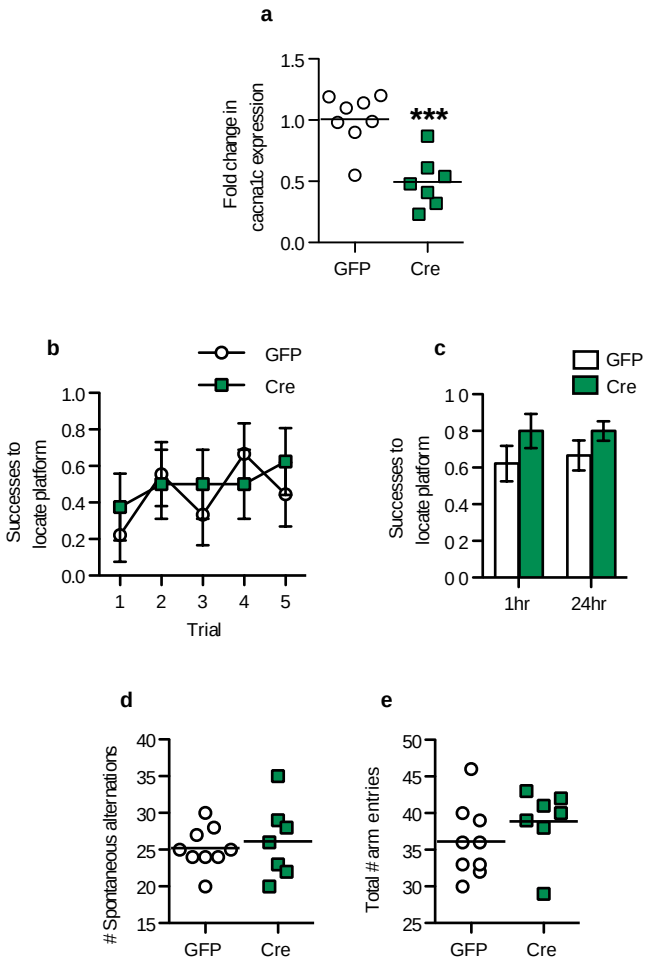

Supplementary Figure 4

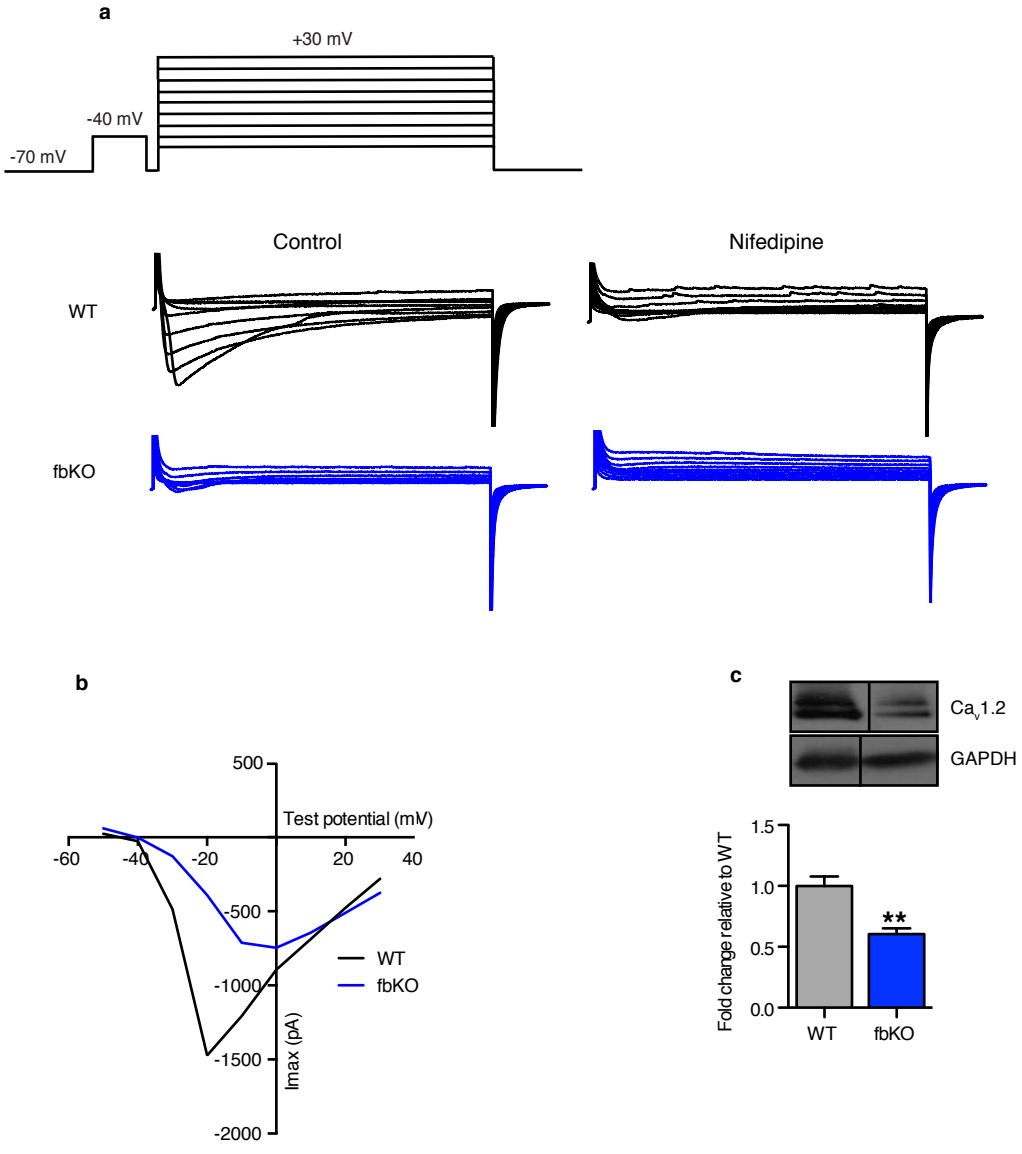

Supplementary Figure 5

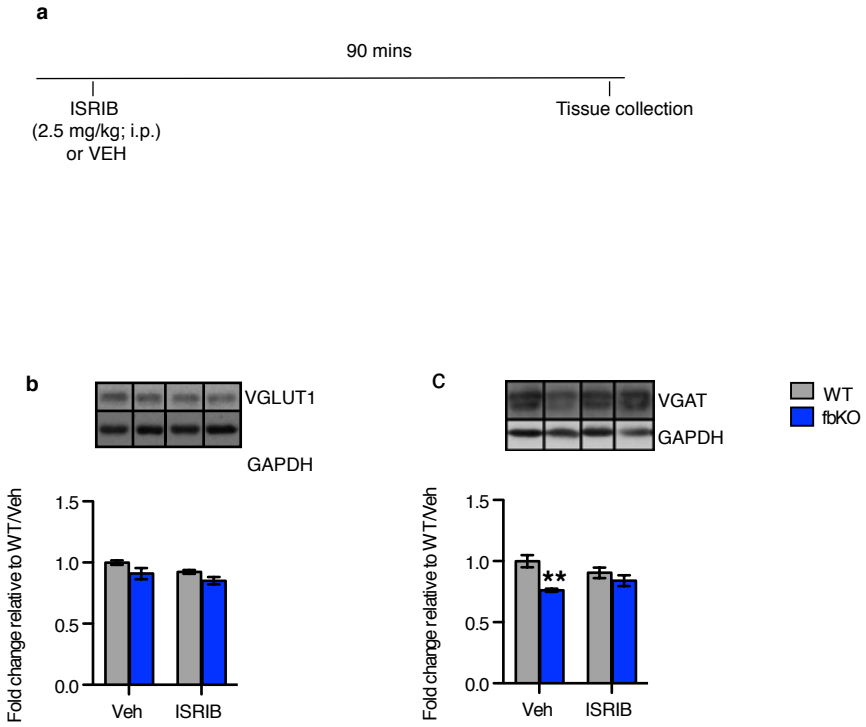

SUPPLEMENTARY FIGURE LEGENDS

Supplementary Figure 1. $Ca_v1.2$ and CaMKII are co-expressed in PFC neurons, present in dendritic shafts and dendritic spines, and are affiliated with the postsynaptic density and extra- and perisynaptic plasma membrane.

(**a**) Electron micrograph showing the soma of a PFC neuron that expresses immunoperoxidase labeling for $Ca_v1.2$ and silver-gold labeling for CaMKII. As shown in the dashed box, labeling for each protein is associated with a Golgi complex (Gc) adjacent to the nucleus (nuc). The Gc is shown at a higher magnification in the insert to better visualize $Ca_v1.2$ (green arrow heads) and CaMKII (red arrows) labeled vesicles. Unlabeled vesicles (gray arrow heads) are shown for comparison. (**b**) A small dendritic shaft shows labeling for both $Ca_v1.2$ and CaMKII (cav-cam-d). This profile illustrates dense immunoperoxidase reaction product for $Ca_v1.2$ within the postsynaptic density (green arrow head) and an immunogold-silver aggregate for CaMKII (red arrow) located near the extrasynaptic plasma membrane. Dendritic spines (us) devoid of postsynaptic $Ca_v1.2$ labeling are seen in the nearby neuropil. **(c)** A dendritic profile and a spine profile are each co-labeled for $Ca_v1.2$ and CaMKII. The dendritic profile (cav-cam-d) shows immunoperoxidase labeling for $Ca_v1.2$ in the postsynaptic density (green arrow head) and also displays an immunogold-silver aggregate near the adjacent perisynaptic region of the plasma membrane (red arrow). The nearby neuropil contains a dually labeled spine (cav-cam-s) showing labeling for $Ca_v1.2$ on the postsynaptic density (green arrow head) and CaMKII beneath this $Ca_v1.2$ labeled structure (red arrow). Scale bars: 500 nm.

Supplementary Figure 2. *Cacna1c* fbKO mice display impaired learning and memory but normal working memory.

(**a**) Compared to WT mice, fbKO mice displayed fewer successes in locating the submerged platform in the Y-maze during training (Two-way ANOVA, main effect of genotype, $F_{1, 75} = 4.841$, $p = 0.0309$; WT n = 9, fbKO n = 8). (**b**) Compared to WT mice, fbKO mice displayed a trend towards fewer successes in locating the submerged platform in the Y-maze at 1 hour (Student's *t*-test, $t(15) = 1.775$, $p = 0.0962$) and significantly lower success at 24 hours (Student's *t*-test with Welch's correction, $t(9) = 2.73$, $p < 0.05$) but not 7 days post-training (WT n = 9, fbKO n = 8). (**c, d**) WT and fbKO mice displayed similar number of spontaneous alternations (**c**) and total arm entries (**d**) during the working memory task in the Y-maze (WT n = 8, fbKO n = 8). *$p < 0.05$ vs WT. Error bars represent mean ± SEM.

Supplementary Figure 3. Knockdown of *cacna1c* in the adult PFC of mice does not impair learning and memory or working memory.

(**a**) Lower *cacna1c* mRNA levels in the PFC of Cre mice (Student's *t*-test, $t(13) = 4.673$, $p = 0.0004$; GFP n = 8, Cre n= 7). (**b, c**) GFP and Cre mice displayed similar level of successes in locating the submerged platform in the Y-maze during training (**b**) and the 1 hour and 24 hour memory tests (**c**; GFP n = 9, Cre n = 8). (**d, e**) GFP and Cre mice displayed similar number of spontaneous alternations (**d**) and total arm entries (**e**) during the working memory task in the Y-maze (GFP n = 8, Cre n = 8). Error bars represent mean ± SEM.

Supplementary Figure 4. *Cacna1c* fbKO mice exhibit reduced amplitude of L-type calcium currents.

(**a**) Pulse protocol used (top) and representative traces (bottom) of L-type calcium channel currents from layer 5 pyramidal neurons of the PFC with the L-type calcium channel blocker nifedipine. (**b**) Current-voltage relationship measured from subfigure a (WT n = 2, fbKO n = 4). (**c**) fbKO mice have significantly lower levels of $Ca_v1.2$ protein in the synaptoneurosomes from the PFC (Student's *t*-test, $t(11) = 4.192$, $p < 0.01$). **p < 0.01 vs WT. Error bars represent mean ± SEM.

Supplementary Figure 5. ISRIB corrects the decreased protein levels of VGAT in the PFC of *cacna1c* fbKO mice

(a) Outline of experimental design. Adult WT and fbKO mice were given a single systemic injection of either ISRIB (2.5 mg/kg, i.p) or vehicle and ninety minutes later sacrificed. (**b**) fbKO and WT mice have similar levels of synaptoneurosomal VGLUT1 in the PFC that remain unaltered with ISRIB treatment (Two-way ANOVA, main effect of genotype, $F_{1, 24} = 8.468$, $p = 0.0077$; main effect of treatment, $F_{1, 24} = 5.679$, $p = 0.0254$). (**c**) Vehicle treated fbKO mice have significantly lower levels of synaptoneurosomal VGAT protein in the PFC compared to WT vehicle mice that is normalized with ISRIB (Two-way ANOVA, main effect of genotype, $F_{1, 24} = 12.63$, $p = 0.0016$; genotype x treatment, $F_{1, 24} = 4.201$, $p = 0.0516$; Bonferroni *post-hoc* test, **p < 0.01 vs WT Veh; Veh n = 6/ genotype, ISRIB n =6/ genotype). Error bars represent mean ± SEM.

SUPPLEMENTARY METHODS

Animals. Homozygous *cacna1c* floxed mice (*cacna1c*$^{fl/fl}$;[1]) were crossed with mice expressing Cre recombinase under the control of the *Camk2a* (calcium/calmodulin-dependent protein kinase II alpha) promoter (*Camk2a*-Cre T29-1;[2] Jackson Laboratories, Bar Harbor, Maine) to generate heterozygous fbKO (Cre$^{+/-}$, *cacna1c*$^{fl/fl}$) mice. Male and female Cre$^{+/-}$, *cacna1c*$^{fl/fl}$ mice were bred to generate homozygous fbKO (Cre$^{+/-}$, *cacna1c*$^{fl/fl}$) and WT (Cre$^{+/-}$, *cacna1c*$^{WT/WT}$) experimental mice. Mice were provided food and water *ad libitum* and maintained on a 12 hour light/dark cycle (from 6 A.M. to 6 P.M.).

Electron Microscopy (EM). Brains from WT mice were processed and dual labeled by immunocytochemistry using immunoperoxidase and immunogold-silver markers[3] as described below. Brains were fixed by transcardial perfusion sequentially with 2 ml of 2% heparin in 0.9% saline (1,000 U/ml) and 50 ml of a fixative consisting of 3.75% acrolein / 2% paraformaldehyde in 0.1 M phosphate buffer (PB; pH 7.4)[3]. Brains were dissected from the cranium and post-fixed in acrolein / paraformaldehyde for 30 minutes[3]. The methods for tissue processing and dual labeling immunocytochemistry using immunoperoxidase and immunogold-silver markers were performed as previously described[3]. Labeling of $Ca_v1.2$ and CaMKII was performed by incubating PFC sections for 48 hour in a cocktail consisting of rabbit anti-$Ca_v1.2$ (1:15,000; antibody generated by Prosci Incorporated, against $Ca_v1.2$ peptide sequence CKYTTKINMDDLQPSENEDKS as previously published[4]) and goat anti-CaMKII-α (1:1000; Abcam, Cambridge, MA) antisera. Characterization of these reagents is as

previously reported[4, 5]. For EM imaging, sections were examined using a Tecnai Biotwin 12 transmission electron microscope (FEI, Hillsboro, OR) interfaced with a digital camera (Advanced Microscopy Techniques, Danvers, MA) using procedures as previously described[6]. Images were collected at magnifications ranging from 10,000-19,000x. Immunoperoxidase labeling was identified by a diffuse brown/black precipitate, while gold-silver labeling was characterized by dense uniformly black granules. Both markers are readily distinguishable by visual inspection. Profiles containing $Ca_v1.2$ and/or CaMKII immunoreactivity were classified as neuronal (soma, dendrites, axons, terminals) or glial based on criteria previously described[7]. Criteria for field selection included good morphological preservation, the presence of immunolabeling in the field, and proximity to the tissue-plastic interface (i.e., the tissue surface) to minimize differences in antisera penetration. For preparation of figures, images were adjusted for contrast and brightness using Adobe Photoshop CS4 software.

Stereotaxic Surgery. Adult mice were anesthetized with a xylazine (20mg/ml) and ketamine (100mg/ml) cocktail, and mounted in a stereotaxic surgical apparatus (David Kopf Instruments, Tujunga, CA). An incision was made in the scalp along the midline, the skin was retracted, and the head was leveled based on the horizontal positions of bregma and lambda. Two holes were formed through the skull using a 25-gauge needle and AAV2/2-GFP or AAV2/2-Cre-GFP (Vector Biolabs, Malvern, PA) was delivered into the PFC with a 2.5ul, 30-gauge Hamilton syringe at a rate of 0.1ul/min for a total volume of 0.8ul/hemisphere. Stereotaxic coordinates for the PFC were anteroposterior (AP): +2.3 mm, mediolateral (MV): ±1.7 mm, dorsoventral (DV): -2.8 mm; angled 30°

toward the midline in the coronal plane, adopted from Paxinos and Franklin[8]. Mice were allowed to recover in their home-cage for five weeks prior to behavioral testing.

Green Fluorescent Protein (GFP) immunohistochemistry. GFP immunocytochemistry was used to confirm placement of surgical injections as described previously[9]. Briefly, animals were anaesthetized with euthasol and perfused transcardially with 4% paraformaldehyde (PFC). Brains were dissected, post-fixed overnight in 4% PFA, and cryo-protected in 30% sucrose at 4°C for at least 72 hours. Brains were sectioned at a thickness of 40μm using a sliding microtome and sections containing the PFC were incubated in chicken anti-GFP (1:5000; Aves Lab Inc., Tigard, OR) primary antibody for 24 hours at 4°C. The sections were rinsed in 0.1M phosphate-buffer (PB) and incubated with donkey anti-chicken Alexa Fluor 488 (1:500; Life Technology, Carlsbad, CA) antibody for 1 hour at room temperature. Sections were imaged using an epifluorescent microscope (Leica DM550B with Leica Application Suite Advanced Fluorescence 3.0.0 build 8134 software, Leica Microsystems, Wetzlar, Germany). Animals with improper bilateral injection placement were excluded from behavioral data analysis.

Behavioral testing.

Three-chambered social approach test. The test apparatus consisted of a white rectangular apparatus measuring 26.5”x16.5”x 9” that was divided into three equal-sized chambers with openings that allowed animals free access to all chambers (Figure 1a). Before the start of the test, the experimental animal was habituated to the central chamber of the apparatus for 5 minutes followed by an additional 5-minute habituation to all three

chambers. Following habituation, the experimental mouse was contained in the center chamber for 1 minute while the experimenter placed an inverted pencil cup containing a never-before-met age-matched male C57BL6/J stranger mouse in one end chamber and a novel object in another pencil cup in the other end chamber. The experimental mouse was then allowed access to all three chambers and "sociability" was tested during a 5 minute test using two individual measures: 1) time in the chamber containing the stranger mouse and the novel object, and 2) time in the contact zones (a 1.5" zone surrounding the pencil cups) of the stranger mouse and novel object. The experiment was recorded using a video-camera mounted above the apparatus and the position of the experimental mouse was tracked using Any-maze software (Stoelting Co.,Wood Dale, IL). All measurements were obtained via automated analyses using AnyMaze (Stoelting Co.,Wood Dale, IL).

Fear conditioning. All experiments were performed in a sound-attenuated box (Coulbourn, Whitehall, PA). On day 1, mice were placed in a mouse shock-chamber (context A) that was scented with 0.1% peppermint odor and presented with five tones (85dB, 30 seconds, with incrementally increasing inter-trial interval (ITI)) that co-terminated with a shock (0.7mA, 1 second). For the cue fear memory test, animals were placed in a novel chamber (context B, circular in shape with white walls and scented with 0.1% lemon odor) and exposed to 5 tones (85dB, 30 seconds, ITI = 30 seconds) during which their freezing was measured. Data is presented as the percent freezing during presentation of each 30-second tone. For the contextual fear memory test, animals were placed back in context A and their freezing to the context was measured for 4.5 minutes. Data is presented as the percent freezing during the entire test period. The experiment

was recorded using FreezeFrame software and the time of freezing was measured via automated analysis using FreezeView (Coulbourn Instruments, Whitehall, PA).

Water-based Y-maze. The Y-maze consisted of three equal sized arms with a 120° angle between each arm (Figure 1g). The maze was filled with water (25-26°C) to a height of approximately 9" and clouded with non-toxic white tempura paint. On day 1, mice were placed in the center of the maze and allowed free access to all arms for a total of 6 minutes. The number of arm entries and the number of triads were recorded to calculate the percent of spontaneous alternations, to measure working memory. On day 2, mice were subjected to 5 training trials to locate a submerged platform in one arm of the Y-maze. This was followed by short- (1 hour) and long-term (24 hour and 7 day) memory tests, each of which consisted of 5 trials. The start position and the location of the platform were randomized across mice used in the behavioral test. However for each mouse the chosen start position and location of the platform remained consistent throughout the entire experiment. During each trial the mouse was allowed free access to the maze for a total of 1 minute and the latency to locate the submerged platform and errors made during each trial were recorded. If the platform was not found after 1 minute, the mouse was picked up and placed on the platform for an additional 15 seconds and then rescued from the platform. Successes for each animal was calculated based on the errors made during each trial. An animal that went into the correct arm (the arm that had the submerged platform) without entering the incorrect arm was given a score of 1 while an animal that went into the incorrect arm before entering the correct arm was given a score of 0. For the memory tests, data is presented as an average of the five trials.

Morris water maze (MWM). MWM was performed as previously published[10] with slight modifications. The maze consisted of a circular stainless steel pool with a diameter of 6' and a depth of 14.5" (Figure 1k) that was filled with water (25-26°C) and clouded with non-toxic white tempura paint. Four different start positions were designated. Spatial cues were placed on the wall one foot from the edge of the pool. The maze was virtually divided into four equal quadrants with one quadrant designated as the "goal" for each individual mouse. The other quadrants were designated as clockwise, counter-clockwise and opposite relative to the goal quadrant. The start position and goal quadrant was randomized across mice used in the behavioral test. On day 1, animals were habituated to the pool for a total of 4 trials of 1 minute each, during which the mouse was placed in the center of the pool and allowed free access throughout the pool. On days 2 through 7, mice received a total of 24 trials (4/ day). During each training trial, the mouse was released from a different start position and allowed to swim for a maximum of 1 minute to locate a submerged platform placed in the goal quadrant. Although the start position for each mouse varied from trial-to-trial, the goal always remained the same throughout the length of the training. Animals that successfully located the submerged platform were rescued from the platform and returned to their home cage; those that failed to locate it within 1 minute were placed on the platform for an additional 15 seconds and then returned to their home cage. During training trials, latency to locate the hidden platform was measured. Probe tests were performed 1 hour (for short-term memory), 24 hours, and 7 days (for long-term memory) post-training. During each probe test, the mice were placed in the pool from the exact opposite end of the designated goal quadrant and the amount of

time the animal spent in the "goal" quadrant compared to that in the other quadrants was measured for a total of 1 minute. During the probe trials, the amount of time the animal spent in the goal quadrant (quadrant that had the submerged platform during training) compared to each of the other quadrants was measured. All trials were recorded using a video-camera mounted above the maze and the position was tracked using Any-maze software (Stoelting Co., Wood Dale, IL).

Electrophysiological methods.

Acute brain slice preparation. Postnatal day (P) 30-P45 mice were anesthetized with isoflurane and decapitated. Brains were dissected and immersed in ice-cold oxygenated (95%O_2 and 5%CO_2) dissection buffer containing (in mM): 83 NaCl, 2.5 KCl, 1 NaH_2PO_4, 26.2 $NaHCO_3$, 22 glucose, 72 sucrose, 0.5 $CaCl_2$, and 3.3 $MgCl_2$. Coronal slices (400 μm) were cut using a vibratome (VT1200S, Leica, Wetzlar, Germany), incubated in dissection buffer for 40 min at 34°C, and then stored at room temperature. All slice recordings were performed at 34°C unless otherwise specified. Slices were visualized using IR differential interference microscopy (DIC; BX51, Olympus, Tokyo, Japan) and a CMOS camera (Orca-Flash4.0LT, Hamamatsu, Japan). Individual cells were visualized with a 60x Olympus water immersion (1.0 NA) objective.

Whole-cell recording. For all experiments, external recording buffer was oxygenated (95%O_2 and 5%CO_2) and contained (in mM): 125 NaCl, 25 $NaHCO_3$, 1.25 NaH_2PO_4, 3 KCl, 25 dextrose, 1 $MgCl_2$, and 2 $CaCl_2$. Patch pipettes were fabricated from borosilicate glass (Sutter Instrument, Novato, CA) to a measured tip resistance of 2-5 MΩ. Signals

were amplified with a Multiclamp 700A amplifier (Molecular Devices, Sunnyvale, CA), digitized with an ITC-18 digitizer (HEKA Instruments Inc., Bellmore, NY) and filtered at 2 KHz. Data were monitored, acquired and in some cases analyzed using AxoGraph X software (Berkeley, CA). Series resistance was monitored throughout the experiments by applying a small test voltage step and measuring the capacitive current. Series resistance was 5~25 MΩ and only cells with <20% change in series resistance and holding current were included for analysis. Liquid junction potential was not corrected.

To measure spontaneous mini excitatory postsynaptic currents (mEPSCs), recording pipettes were filled with an internal solution containing (in mM): 125 potassium gluconate (or CsCl for recording mIPSCs), 10 KCl, 10 HEPES, 4 Mg-ATP, 0.3 Na-GTP, 0.1 EGTA, 10 phosphocreatine, 0.05% biocytin, adjusted to pH 7.3 with KOH and to 278 mOsm with double-distilled H_2O. Spontaneous mEPSCs were measured at -80 mV, in the presence of the $GABA_A$ receptor blocker SR-95531 (Gabazine, 5μM, Abcam, Cambridge, MA) to isolate α-amino-3-hydroxy-5-methyl-4-isoxazolepropionic acid receptor (AMPAR)-mediated events. Spontaneous mIPSCs were measured at 0 mV. To detect events, a variable amplitude template was slid through the 180s chart recordings[11]. The parameters of the template, including amplitude, 10-90% rise time, and decay time, were determined based on an average of real events as well as previously reported values. The detection threshold was 3 to 7 times of the noise standard deviation, and events with large baseline error were rejected. Data analysis was performed using Axograph X built-in analysis and IGOR Pro software (Wavemetrics) on a Macintosh computer.

Molecular methods.

SUnSET. Adult mice were anesthetized with an isoflurane vaporizer (at 1.5%) and mounted in a stereotaxic surgical apparatus (David Kopf Instruments, Tujunga, CA). The head was leveled based on the horizontal positions of bregma and lambda, and an incision was made in the scalp along the midline. The skin was retracted and a single hole was formed through the skull using a 25-gauge needle using the following coordinates for the lateral ventricle (AP: -0.2; ML: -1.0; DV: -2.4). Puromycin (Sigma, St. Louis, MO), at a concentration of 10µg/µl, was injected into the lateral ventricle at a rate of 0.4µl/min for a total volume of 2.5ul. Animals were sutured and allowed to recover. For basal protein synthesis measurments, animals were euthanized one-hour post injection, and the PFC, somatosensory cortex and hippocampus were dissected on dry ice. For general protein synthesis measurements with acute ISRIB treatment, ISRIB was injected intraperitoneally at the start of puromycin infusion and animals were euthanized 90 minutes later. Western blot analysis using total fractions was performed as described below. 100µg total protein was separated on a 10% gel and probed with an antibody against puromycin (#MABE343, Millipore, Temecula, CA) at a dilution of 1:500 for the primary antibody and 1:5000 for the secondary. Tubulin was used as a loading control at a dilution of 1:60,000 for the primary and 1:100,000 for the secondary.

Subcellular fractionation and immunoblotting. Adult mice were decapitated, brains were dissected, and crude dissections of the PFC were performed using a 17-gauge stainless steel stylet. For total protein lysates, tissue was sonicated in SDS lysis buffer (1%SDS in 1X TE, pH 7.4) containing protease and phosphatase inhibitors as previously

208 described[12]. Synaptoneurosomes were generated as previously published[13]. Briefly, tissue
209 was homogenized in 0.3M sucrose/ 0.01mM HEPES buffer containing protease and
210 phosphatase inhibitors and centrifuged at 1000xg. The supernatant was spun again at
211 1000xg. The obtained supernatant was spun at 12,000xg and the resulting pellet was
212 resuspended in 4mM HEPES/ 1mM EDTA buffer and used as the synaptoneurosome
213 fraction. Protein concentrations were determined using the BCA assay and protein lysates
214 were separated on a 10% SDS gel along with a Kaleidoscope-prestained protein standard
215 (Bio-Rad, Hercules, CA). Blots were blocked in 5% non-fat dry milk for 1 hour and
216 incubated in primary antibody (see Supplementary Table 1) for 12-48 hours on a shaker
217 at 4°C. Incubation in secondary antibody (see Supplementary Table 1) was performed at
218 room temperature for 1 hour in horseradish peroxidase-linked IgG conjugated antibody.
219 Membranes were visualized using Western Lightning Chemiluminescence solution
220 (Perkin Elmer Life Science, Boston, MA) and optical density was analyzed using NIH
221 Image (NIH, Bethesda, MD). Proteins were normalized to either GAPDH or tubulin,
222 which was used as a loading control. Data in figures 3a and 3e were analyzed from
223 images obtained with the ChemiDoc Imaging System (Bio-Rad, Hercules, CA). All other
224 western analyses were done using X-ray film.
225
226 **BDNF ELISA.** Tissue was homogenized in lysis buffer containing (150mM NaCl, 1%
227 Triton X-100, 25mM HEPES, 2mM NaF) and incubated on a rotating nutator at 4°C for 1
228 hour. Homogenized tissue was centrifuged at 20,000xg and the supernatant containing
229 total protein was quantified using the BCA protein assay. Mature BDNF protein was

measured using the BDNF Emax ImmunoAssay System (Promega, Madison, WI) as previously published[14].

Quantitative Real-Time PFC (QPCR). RNA was extracted and QPCR was performed as previously described[15]. *Cacna1c* (QuantiTect Primer assay QT00150752; Qiagen) mRNA levels were measured using mRNA-specific primers and normalized to *GapDH* (QuantiTect Primer assay QT01658692; Qiagen). All samples were performed in triplicate, and the values were averaged.

REFERENCES

1. Moosmang S, Haider N, Klugbauer N, Adelsberger H, Langwieser N, Müller J *et al.* Role of hippocampal Cav1.2 Ca2+ channels in NMDA receptor-independent synaptic plasticity and spatial memory. *The Journal of neuroscience : the official journal of the Society for Neuroscience* 2005; **25**(43)**:** 9883-9892.

2. Tsien JZ, Chen DF, Gerber D, Tom C, Mercer EH, Anderson DJ *et al.* Subregion- and cell type-restricted gene knockout in mouse brain. *Cell* 1996; **87**(7)**:** 1317-1326.

3. Glass MJ, Wang G, Coleman CG, Chan J, Ogorodnik E, Van Kempen TA *et al.* NMDA Receptor Plasticity in the Hypothalamic Paraventricular Nucleus Contributes to the Elevated Blood Pressure Produced by Angiotensin II. *The Journal of neuroscience : the official journal of the Society for Neuroscience* 2015; **35**(26)**:** 9558-9567.

4. Tippens AL, Pare JF, Langwieser N, Moosmang S, Milner TA, Smith Y *et al.* Ultrastructural evidence for pre- and postsynaptic localization of Cav1.2 L-type Ca2+ channels in the rat hippocampus. *J Comp Neurol* 2008; **506**(4)**:** 569-583.

5. Gan JO, Bowline E, Lourenco FS, Pickel VM. Adolescent social isolation enhances the plasmalemmal density of NMDA NR1 subunits in dendritic spines

of principal neurons in the basolateral amygdala of adult mice. *Neuroscience* 2014; **258:** 174-183.

6. Beckerman MA, Van Kempen TA, Justice NJ, Milner TA, Glass MJ. Corticotropin-releasing factor in the mouse central nucleus of the amygdala: ultrastructural distribution in NMDA-NR1 receptor subunit expressing neurons as well as projection neurons to the bed nucleus of the stria terminalis. *Exp Neurol* 2013; **239:** 120-132.

7. Peters A, Palay SL, Webster HD. The fine structure of the nervous system. 1991.

8. Paxinos G, Franklin KBJ. *The Mouse Brain in Stereotaxic Coordinates. 2nd Edition.* Academic Press2001.

9. Lee AS, Ra S, Rajadhyaksha AM, Britt JK, De Jesus-Cortes H, Gonzales KL *et al.* Forebrain elimination of cacna1c mediates anxiety-like behavior in mice. *Mol Psychiatry* 2012; **17**(11)**:** 1054-1055.

10. Vorhees CV, Williams MT. Morris water maze: procedures for assessing spatial and related forms of learning and memory. *Nat Protoc* 2006; **1**(2)**:** 848-858.

11. Clements JD, Bekkers JM. Detection of spontaneous synaptic events with an optimally scaled template. *Biophys J* 1997; **73**(1)**:** 220-229.

12. Tropea TF, Kabir ZD, Kaur G, Rajadhyaksha AM, Kosofsky BE. Enhanced dopamine D1 and BDNF signaling in the adult dorsal striatum but not nucleus accumbens of prenatal cocaine treated mice. *Front Psychiatry* 2011; **2:** 67.

13. Knackstedt LA, Moussawi K, Lalumiere R, Schwendt M, Klugmann M, Kalivas PW. Extinction training after cocaine self-administration induces glutamatergic plasticity to inhibit cocaine seeking. *The Journal of neuroscience : the official journal of the Society for Neuroscience* 2010; **30**(23)**:** 7984-7992.

14. Kabir ZD, Katzman AC, Kosofsky BE. Molecular mechanisms mediating a deficit in recall of fear extinction in adult mice exposed to cocaine in utero. *PloS one* 2013; **8**(12)**:** e84165.

15. Schierberl K, Hao J, Tropea TF, Ra S, Giordano TP, Xu Q *et al.* Cav1.2 L-type Ca^{2+} channels mediate cocaine-induced GluA1 trafficking in the nucleus accumbens, a long-term adaptation dependent on ventral tegmental area Ca(v)1.3 channels. *The Journal of neuroscience : the official journal of the Society for Neuroscience* 2011; **31**(38)**:** 13562-13575.

Supplementary Table 1. List of antibodies used for immunoblotting.

Antibody	Company	Cat #	Dilutions (primary/ secondary)	Secondary	Mol Wt (kDa)
mTOR	Cell Signaling, Danvers, MA	2972	1:1000/ 1:5000	HRP α Rb	289
P-mTOR S2448	Cell Signaling, Danvers, MA	2971	1:1000/ 1:5000	HRP α Rb	289
4EBP1	Cell Signaling, Danvers, MA	9459	1:1000/ 1:5000	HRP α Rb	15-25
P-4EBP1 T37/46	Cell Signaling, Danvers, MA	9459	1:1000/ 1:5000	HRP α Rb	15-25
eIF4B	Cell Signaling, Danvers, MA	3592	1:1000/ 1:5000	HRP α Rb	80
P-eIF4B S422	Cell Signaling, Danvers, MA	3591	1:1000/ 1:5000	HRP α Rb	80
eEF2	Cell Signaling, Danvers, MA	2332	1:1000/ 1:5000	HRP α Rb	95
P-eEF2 T56	Cell Signaling, Danvers, MA	2331	1:1000/ 1:5000	HRP α Rb	95
rpS6	Cell Signaling, Danvers, MA	2217	1:1000/ 1:5000	HRP α Rb	32
P-rpS6 S235/236	Cell Signaling, Danvers, MA	2211	1:500/ 1:5000	HRP α Rb	32
P-rpS6 S240/244	Cell Signaling, Danvers, MA	2215	1:1000/ 1:5000	HRP α Rb	32
eIF2α	Cell Signaling, Danvers, MA	9722	1:1000/ 1:5000	HRP α Rb	38
P-eIF2α	Cell Signaling, Danvers, MA	3398	1:1000/ 1:5000	HRP α Rb	38

S51					
GAPDH	Abcam, Cambridge, MA	ab22555	1:20,000/ 1:40,000	HRP α Rb	37
Tubulin	Sigma, St. Louis, MO	T5168	1:10,000/ 1:30,000	HRP α Ms	50
$Ca_v1.2$	Alomone Labs, Jerusalem, Israel	AGP-001	1:300/ 1:5000	HRP α Guinea pig	250
VGlut	Neuromab, Davis, CA	Clone N28/9	1:1000/ 1:5000	HRP α Rb	52
VGat	Synaptic Systems, Germany	131 002	1:1000/ 1:5000	HRP α Rb	57